SUPPLEMENTAL MATERIAL

Detailed Methods

Animal Studies

Generation of PGC-1$\alpha^{-/-}\beta^{f/f/MCK\text{-}Cre}$ mice was previously described.[1] Briefly, PGC-1$\beta^{f/f}$ mice[2] were crossed with mice expressing Cre under control of a MCK promoter[3] to achieve muscle-specific deletion of PGC-1β. These mice in turn were crossed to obtain mice homozygous for the loss of PGC-1α[4] and the PGC-1β flox allele (PGC-1$\alpha^{-/-}\beta^{f/f}$ mice), with and without MCK-Cre. PGC-1$\beta^{f/f}$ and PGC-1$\beta^{f/f/MCK\text{-}Cre}$ mice were generated from the same breeding pairs, while PGC-1$\alpha^{-/-}\beta^{f/f}$ and PGC-1$\alpha^{-/-}\beta^{f/f/MCK\text{-}Cre}$ mice were generated from a different set of breeding pairs.

The tamoxifen-inducible, heart-specific, double PGC-1α and β knockout mouse (PGC-1$\alpha^{-/-}\beta^{f/f/MerCre}$) was generated by the same breeding scheme as the PGC-1$\alpha^{-/-}\beta^{f/f/MCK\text{-}Cre}$ mice described above, using the mutated estrogen receptor-Cre recombinase fusion protein under control of alpha-myosin heavy chain (MHC) promoter (MHC-MerCre, provided by Dr. Jeff Molkentin, U. of Cincinnati), to cause a cardiac-specific deletion of PGC-1β.

At 2 months of age, PGC-1$\alpha^{-/-}\beta^{f/f/MerCre}$ mice were injected on two sequential days with 50mg/kg/day of tamoxifen (T5648, Sigma) dissolved in sunflower seed oil (S5007, Sigma) to translocate Cre into the nucleus and create adult PGC-1α/β deficient mice (PGC-1αβ$^{-/-}$). The following control animals were used for the adult model experiments. For wild-type control mice (PGC-1αβ$^{+/+}$), a mix of tamoxifen injected PGC-1$\beta^{f/f}$ and vehicle injected PGC-1$\beta^{f/f/MerCre}$ mice were used. For PGC-1α single knockout mice (PGC-1$\alpha^{-/-}$), a mix of tamoxifen injected PGC-1$\alpha^{-/-}\beta^{f/f}$ and vehicle injected PGC-1$\alpha^{-/-}\beta^{f/f/MerCre}$ mice were used unless otherwise specified. All PGC-1β single knockout mice (PGC-1$\beta^{-/-}$) were tamoxifen injected PGC-1$\beta^{f/f/MerCre}$ mice. All endpoint measurements were made 1 month after injection unless otherwise noted.

Echocardiography

Serial ultrasound examination of the heart was performed non-invasively using a Vevo2100 Microultrasound System (VisualSonics Inc, Toronto, Ontario, Canada) as we have described.[2] 1 week old mice were lightly anesthetized with isoflurane (3% induction and 1% maintenance). Adult mice (4 and 8 weeks) were anesthetized with intraperitoneal injection of 0.01 ml/g of 2% Avertin (tribromoethanol). Importantly, low-dose Avertin does not exert significant negative inotropic or chronotropic effects. Hair was removed from the anterior chest in adult mice using chemical hair remover and the animals were placed on a warming pad in a left lateral decubitus position to maintain normothermia (around 37^{o}C). Ultrasound gel was applied to the chest. Cursory examination of cardiac structure and function under physiologic conditions was obtained by hand-held manipulation of the ultrasound transducer (30-60 MHz) to obtain 2D and 2-D guided M-mode images. Physiologic parameters including heart rate, respiratory rate, and core body temperature were continuously monitored by a built-in monitoring system. Care was taken to maintain adequate contact while avoiding excessive pressure on the chest. All the echocardiographic images were analyzed by the analysis software of Vevo 2100. Measurement of wall thickness and luminal diameters (interventricular septum, IVS; left ventricle posterior wall, LVPW; left ventricle internal luminal diameters, LVID) were made from M-mode images of the left ventricle in both systole (s) and diastole (d) following the guidelines of American Society of Echocardiography.[5] Left ventricular fractional shortening (LV FS%) and ejection fraction (EF %), a measure of systolic function, were calculated as: LV FS(%)= [(LVIDd-LVIDs/LVIDd)x100];[6] Ejection fraction was calculated according to Teichholz, (LV-EF%)=[(LVEDV-LVESV/LVEDV)]x100;[7] Left ventricular mass (LVM) was calculated as: [(IVSd+LVIDd+LVPWd)3-(LVIDd)3]x1.04.[6]

Mitochondrial respiration studies

For the PGC-1$\alpha^{-/-}\beta^{f/f/MCK\text{-}Cre}$ mice and their controls, respiratory function was assessed for mitochondria isolated from combined left and right cardiac ventricles using a previously described isolation protocol.[8,9] Two hearts from 4 week-old sex matched mice were pooled per sample. Respiration measurements were conducted using an optical probe (Oxygen FOXY Probe, Ocean Optics) as described previously.[2] The respiration of the mitochondrial isolate containing 0.3 mg protein was measured at 37°C using an optical probe (Oxygen FOXY Probe, Ocean Optics). The respiration buffer[10] contained the following (in mM): 125 KCl, 20 HEPES, 3 Mg-acetate, 5 KH_2PO_4, 0.4 EGTA, and 0.3 DTT, pH 7.1 at 25°C, with 2 mg/ml BSA added. For palmitoyl-l-carnitine (PC) respiration, the respiration buffer also contained 20 μM PC and 5 mM malate. For pyruvate respiration, the respiration buffer contained 10 mM pyruvate and 5 mM malate. Following measurement of basal respiration, state 3 (maximal ADP-stimulated) respiration was determined by exposing the mitochondria to 1 mM ADP. Uncoupled respiration was evaluated following addition of oligomycin (1 μg/mL) to inhibit ATP synthase. Respiration rates were expressed as nanomoles of O_2 per minute per milligram of mitochondrial protein.

For the PGC-1$\alpha^{-/-}\beta^{f/f/Mercre}$ mice and their controls, mitochondrial function was assessed by measuring rates of O_2 consumption (OCR) in pmoles O_2/min using a XF24 Extracellular Flux Analyzer (Seahorse Bioscience). Isolated mitochondria (4ug/well) in 1X MAS (70mM Sucrose, 220mM Mannitol, 5mM KH_2PO_4, 5mM $MgCl_2$, 2mM HEPES, 1mM EGTA, 0.1% Fatty Acid Free BSA, pH7.2) were transferred to a 24-well plate. Substrates [pyruvate (5mM)/Malate (5mM)] were added to the well. During the OCR measurement, the compounds in 1 X MAS were injected as follows: Port A, 50ul of 40mM ADP; Port B, 55ul of 10ug/ml Oligomycin; Port C, 60ul of 20uM FCCP; Port D, 65ul of 15ug/ml antimycin A.

Electron microscopy

For electron microscopic (EM) studies, mice were euthanized, cardiac tissue (cardiac papillary muscle for adult, and whole heart for neonates and 1 week-old pups) was harvested, and immediately immersed in Karnovsky's fixative (2% glutaraldehyde, 1% paraformaldehyde, and 0.08% sodium cacodylate) as previously described.[2] For neonates and 1 week-old pups, the left ventricular (LV) free wall was dissected postfixation. All samples were postfixed in 1% osmium tetroxide, embedded in Poly Bed plastic resin, and sectioned for electron microscopy by the Electron Microscopy Core Facility at Washington University School of Medicine. Electron micrographs were collected on the JEM-1011 electron microscope at the University of Central Florida and on the Philips Morgagni transmission electron microscope at the Sanford-Burnham Medical Research Institute (SBMRI) at Lake Nona.

Histological analysis

Masson's Trichrome staining and Caspase staining was performed by the Histology Core at Sanford-Burnham Medical Research Institute at Lake Nona. The tissues were fixed with 10% buffered formalin overnight, dehydrated in 70% ethanol, and embedded in paraffin from which 6-μm sections were prepared. Masson's Trichrome staining was performed using the Prisma automated slide stainer (Sakura Finetek) with G2 coverslipper. HALO software was used to quantitate the area of each field that is covered by blue staining vs. the area of the field covered by red staining. Three to eight fields per group were used. Caspase staining was performed using Cleaved Caspase 3 (Asp175) antibody (Cell Signaling #9661). Images were taken on a Nikon 80i Upright Microscope with a DS F-i1 2560x1920 CCD camera, using a Plan Fluor 10x 0.3 WD 16 DIC L/N1 or Plan Fluor 20x 0.5 WD 2.1 DIC M/N2 objective.

RNA analyses

Total RNA was isolated from cardiac tissue using the RNAzol method (Tel-Test)[2] and from cultured cells using the RNAqueous RNA isolation kit (Ambion) per the manufacturer's instruction. Real-time qRT-PCR was performed using the Stratagene MX3005P detection system and reagents supplied by Stratagene. Specific oligonucleotide primers for target gene sequences are listed in Online Table I. Arbitrary units of target mRNA were corrected to expression of *36b4*.

Promoter scanning and gene expression array studies

The promoter regions for mitofusin 1 (*Mfn1*) mitofusin 2 (*Mfn2*), opticatrophy (*Opa1*), dynamin-related protein 1 (*Drp1*), and fission protein 1 (*Fis1*) were retrieved from the DataBase of Transcriptional Start Sites (-2000 bp to + 500bp). All the alternative promoters were also retrieved. The estrogen-related receptor α (ERRα) motif profile was downloaded from the Transfac database 7.0 (public version). ERRα binding consensus sites were identified within the promoters listed above using visual scans in Vector NTI (Invitrogen), combined with TF searches using Alggen-Promo and Clover[11] software. Conservation between species was determined using "blat" in the UCSC genome database.

Total RNA isolated from cardiac biventricle of 12-week-old PGC-1$\alpha^{-/-}\beta^{f/f/MerCre}$ ($\alpha\beta^{-/-}$) and PGC-1$\alpha^{-/-}$ ($\alpha^{-/-}$) littermates was used for gene expression array studies performed as previously described.[12] The Analytical Genomics Core of Sanford-Burnham Medical Research Institute at Lake Nona performed hybridization to Affymetrix Mouse Gene 1.0 ST array. Five independent samples were analyzed. The Affymetrix probe level data was processed using Robust Multi-Array Analysis (RMA) as implemented in the *affy* package to obtain normalized summary scores of expression for each probe set on each array. *EBarrays* was used to identify genes differentially expressed between $\alpha\beta^{-/-}$ and $\alpha^{-/-}$ hearts.[13,14] The list of genes with posterior probabilities of differential expression greater than 0.95 (expected FDR less than 5%) was considered a regulated gene. For pathway analysis, the filtered data sets were uploaded into Ingenuity Pathway Analysis (IPA) software and biopathways were reviewed using the canonical pathways defined by IPA.

Cardiac myocyte cell culture

Ventricles were removed from 0.5 day old SD rats, minced, and digested 16-20 hours in 500ug/ml trypsin at 4°C. After trypsin inhibition, the tissue was subsequently digested in 300U/ml collagenase (Worthington Biochemical Corporation) for 45 min at 37°C. After mechanical disruption and straining, the cells were pooled in Dulbecco's modified Eagle's medium containing 10% horse serum, 5% fetal calf serum, 0.10 mM 5-bromo-2´-deoxyuridine, 2 mM L-glutamine and plated into 6 well plates pre-treated with gelatin (about 800k cells per well of a 6 well plate). After 24 hours, the cell medium was switched to serum-free Dulbecco's modified Eagle's medium containing 0.10 mM 5-bromo-2′-deoxyuridine, 10 μg/ml insulin, 10 μg/ml transferrin (Sigma), 1 mg/ml fatty acid-free BSA, and 2 mM L-glutamine.

Adenoviral infection

The adenoviral shRNA vectors for PGC-1α,[15] PGC-1β[16] and ERRα[17] were generous gifts from Dr. Montminy (The Salk Institute), Dr. Spiegelman (Harvard University) and Dr. McDonnell (Duke University) respectively. The adenoviral expression vectors for PGC-1α and PGC-1β overexpression were previously described.[2] H9c2 cells were infected with adenovirus 4 days after differentiation and harvested 40-48 hours post-infection. Primary neonatal rat cardiac myocytes (NRCM) were infected with adenovirus 24 hours after differentiation and harvested 72 hours post-infection. The following adenoviral vectors encoding microRNAs were generated by the Zorzano Lab using the method previously described for Ad-miR2Mfn2:[18] Ad-miRct (encoding for a control miRNA), Ad-miR1Opa1 (encoding for 2 miRNAs against Opa1) and Ad-miR1Mfn1 (encoding 2 miRNAs against Mfn1).

Cell transfection and luciferase reporter assays

pcDNA3.1-myc/his.PGC-1α[19,20] and pcDNA3.1-ERRα,[28] and pCATCH-PGC-1β[21] have been described previously.

The mouse *Mfn1* (mMfn1) gene promoter deletion series was generated by PCR amplification from C57BL/6J genomic DNA followed by cloning into the pGL3 Basic firefly luciferase reporter plasmid (Promega, Madison, WI) using Kpn1 and HindIII sites. The following forward primers: 5′-AGTGCTCAGGAATACAAGAATG-3′ (mMfn1.Luc.$^{-}$2996/$^{+}$492); 5′-AGAGATGCCAAGGCAGGAACTGA-3′ (mMfn1.Luc.$^{-}$2299/$^{+}$492, and mMfn1.Luc.$^{-}$2299/$^{+}$70). The following reverse primers were used: 5'-CTTGAAGCCTTCCTTCATGCC-3' (mMfn1.Luc.$^{-}$2996/$^{+}$492 and mMfn1.Luc.$^{-}$2299/$^{+}$492); 5'-GAGCTGTGGTTGCTGGGT-3' (mMfn1.Luc.$^{-}$2299/$^{+}$70). The $(Mfn1ERR\text{-}RE)_2$.TK.Luc and $(Mfn1ERR\text{-}RE)_{2mut}$.TK.Luc plasmids were constructed by ligation of

annealed oligonucleotides (wt sense strand 5'-GATCCACGTCCGGGGTGACCTTCGAGCTCCGGACG -3'; mut sense strand 5'-GATCCACGTCCGGGGTGATTTTCGAGCTCCGGACG-3') into the BamH1 site upstream of the thymidine kinase (TK) promoter of the pGL2-TK.Luc reporter plasmid. The sequence is based on the conserved ERRα site identified +110 downstream of the *Mfn1* transcription start site.

Transient transfections in C2C12 and 10T1/2 cells were performed using Attractene (Qiagen) per the manufacturer's protocol. Per well of 24 well plate, 330 ng of reporter was cotransfected with 133 ng or 33 ng of nuclear receptor expression vectors (for PGC-1α and ERRα respectively), and 33 ng of CMV promoter-driven *Renilla* luciferase (pRL-CMV, Promega) to control for transfection efficiency. Transfections were done 24 hours after cells were plated. C2C12 cells were switched to differentiation media 24 hours after transfection. 96 hours after transfection for C2C12 cells, and 24 hours after transfection for 10T1/2 cells, luciferase assay was performed using Dual-Glo (Promega) according to the manufacturer's recommendations. All transfection data are presented as the mean ± SEM for at least three separate transfection experiments done in triplicate.

Chromatin immunoprecipitation (ChIP) assays

ChIP assays were performed as described.[22,23] Briefly, differentiated H9c2 myotubes were cross-linked with 1% formaldehyde (10 min), and cells were collected and lysed. Chromatin fragmentation was performed by sonication using a Bioruptor (Diagenode). Sheared protein-DNA complexes were immunoprecipitated by using anti-ERRα,[22] anti-PGC-1α,[22,24] or Rabbit IgG control (Sigma). Following reversal of cross-linking, DNA was isolated (QIAquick PCR purification kit, Qiagen). Isolated fragments were amplified by PCR (Stratagene MX3005P detection system) to detect the enrichment of amplicons corresponding to a 100-bp region encompassing the ERR response element of the *rMfn1* gene promoter or a 190-bp region of a distal region of the *rGLUT4* gene (negative control). Specific oligonucleotide primers for target regions are listed in Online Table I. Quantitative analysis was performed by the standard curve method and normalized to IgG control.

Antibodies and Western immunoblotting studies

Western immunoblotting studies were performed with cardiac tissue lysates as previously described.[25] Detection was performed by measuring the chemiluminescent signal as assayed by SuperSignal Ultra (Pierce). Band intensities were quantified using the ChemiDoc (Bio-Rad) or FluorChemQ (Alpha Innotech). The following antibodies were used: Mouse monoclonal anti-DLP1 (DRP-1) (BD Transduction Laboratories #611112); Mouse monoclonal anti-OPA1 (BD Transduction Laboratories #612606); Rabbit polyclonal anti-Mfn2 was generated by the Zorzano lab; Rabbit polyclonal anti-Fis1 (BioVision #3491R-100); Chicken polyclonal anti-Mfn1 (Abnova #PAB12166); VDAC/porin (Abcam #ab15895); S6 ribosomal protein (S6RP) (Cell Signaling Technology #2217S); Complex I subunit 8 kDa (MitoSciences #MS109); Complex II 70kDa Fp subunit (Invitrogen #459200); COX IV (Abcam #ab14744).

Cell culture

H9c2, C2C12, and 10T1/2 cells were maintained at 37°C under 5% CO_2 in Dulbecco's modified Eagle's medium (DMEM) supplemented with 10% fetal bovine serum (FBS). For experiments requiring myotube formation, C2C12 or H9c2 were re-plated onto gelatin-coated plates and maintained for 4-6 days in 2% horse serum or 1% FBS respectively. H9c2 and C2C12 myotubes were infected at a multiplicity of infection sufficient to infect >95% of the cells based on GFP fluorescence with minimal cell death.

Cardiac myocytes were prepared from 0.5-day-old Crl:CD(SD) rats using the Neonatal Cardiomyocyte Isolation System (Worthington Biochemical Corporation) according to the manufacturer's directions as described.[26]

Statistical analyses

Data were analyzed by Student's *t*-test (two-tailed), t-test using the Holm-Sidak method (% fibrosis), Log-rank (% survival), or one-way ANOVA coupled to a Fisher's least significant difference (LSD) post-hoc test as appropriate. Data represent the mean ± standard error of the mean (SEM), with a statistically significant difference defined as a value of $p < 0.05$.

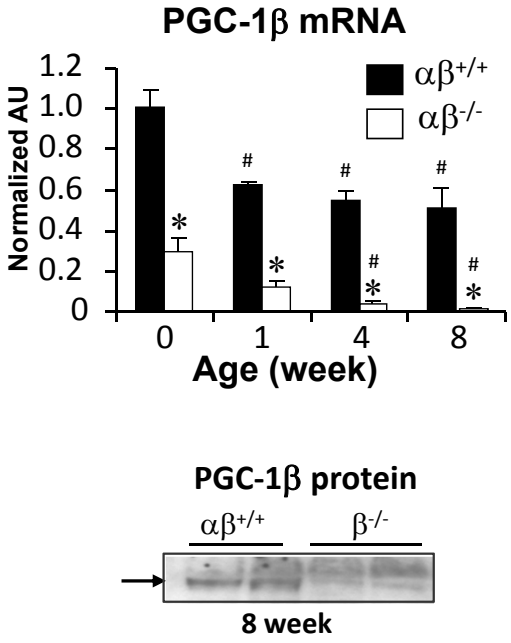

Online Figure I. Evidence for disruption of PGC-1β gene expression in PGC-1α$^{-/-}$β$^{f/f/MCK-Cre}$ heart. PGC-1β mRNA levels determined by qRT-PCR from heart at several age points in PGC-1β$^{f/f}$ ($\alpha\beta^{+/+}$) vs. PGC-1α$^{-/-}$β$^{f/f/MCK-Cre}$ ($\alpha\beta^{-/-}$) mice. *p<0.05 relative to $\alpha\beta^{+/+}$; #p<0.05 relative to DOB (week 0) of the corresponding genotype. A representative Western blot using a PGC-1β antibody is shown at the bottom.

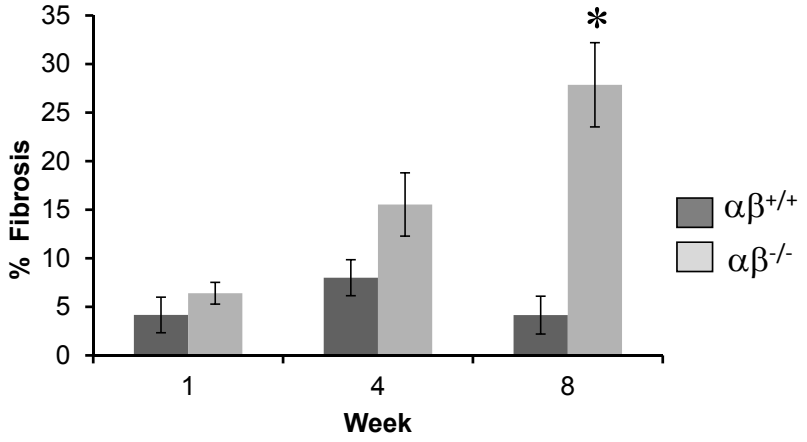

Online Figure II. Quantification of fibrosis in PGC-1α$^{-/-}$β$^{f/f/MCK-Cre}$ hearts. The percent of tissue exhibiting fibrosis was determined using Masson's trichrome staining. Quantification of the fibrotic areas was conducted using Halo software (see Supplemental Methods). The area of fibrotic tissue (blue stain) was calculated as a percent of the entire field of tissue (% Fibrosis). *$p<0.05$ compared to αβ$^{+/+}$.

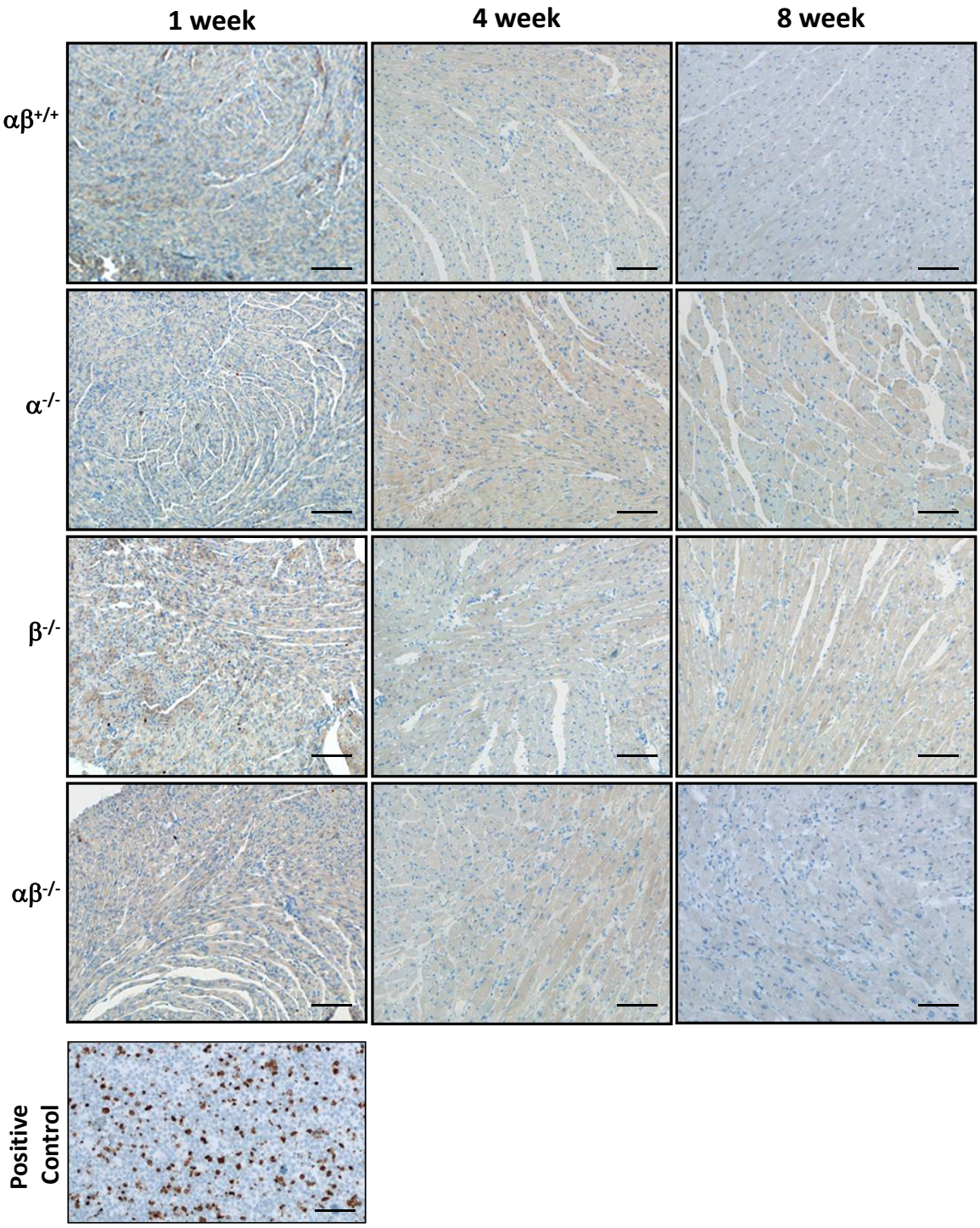

Online Figure III. Caspase staining of PGC-1α$^{-/-}$β$^{f/f/MCK-Cre}$ heart. Representative histologic images of myocardial LV sections from 1, 4, and 8 week old PGC-1β$^{f/f}$ (αβ$^{+/+}$), PGC-1α$^{-/-}$(α$^{-/-}$), PGC-1β$^{f/f/MCK-Cre}$ (β$^{-/-}$) and PGC-1α$^{-/-}$β$^{f/f/MCK-Cre}$ (αβ$^{-/-}$) mice stained using a cleaved Caspase 3 (Asp175) antibody. Etoposide-treated Jurkat cells are shown as a positive control. Scale bars shown are 100 μm.

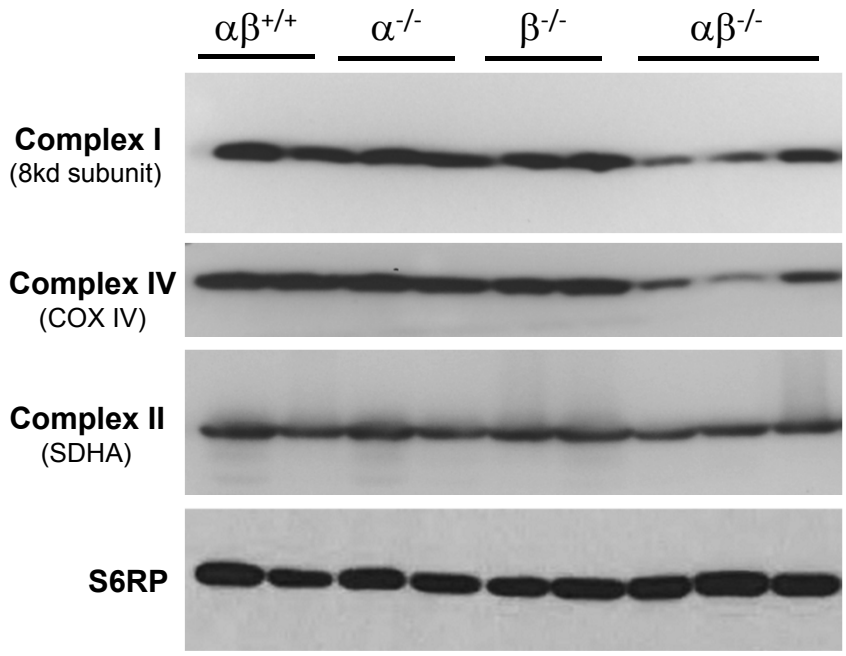

Online Figure IV. Reduced levels of Complex I and IV subunits in PGC-1$\alpha^{-/-}\beta^{f/f/MCK\text{-}Cre}$ hearts.
Representative Western blot analyses performed using protein extracts prepared from 8 week-old mouse heart ventricle tissue homogenate from genotypes denoted at the top. S6 ribosomal protein (S6RP) was used as a non-mitochondrial protein loading control.

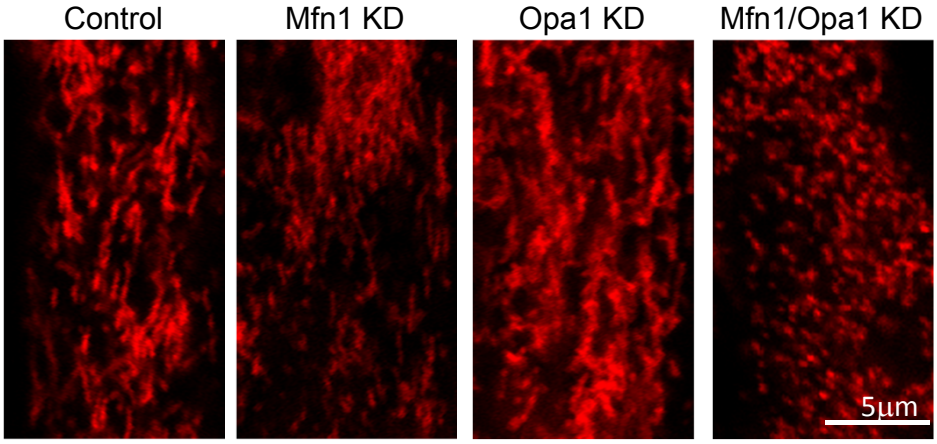

Online Figure V. Opa1 and Mfn1 are required for maintaining normal mitochondrial morphology in C2C12 myotubes. C2C12 myocytes were transduced with adenovirus encoding microRNAs that target Opa1 (78% decrease) and *Mfn1* (66% decrease) prior to differentiation followed by imaging with confocal microscopy after 3 days of differentiation. MitoTracker Red was used to stain the mitochondria. A single representative Z slice is shown. Note the marked fragmentation in the *Mfn1*/*Opa1* KD condition.

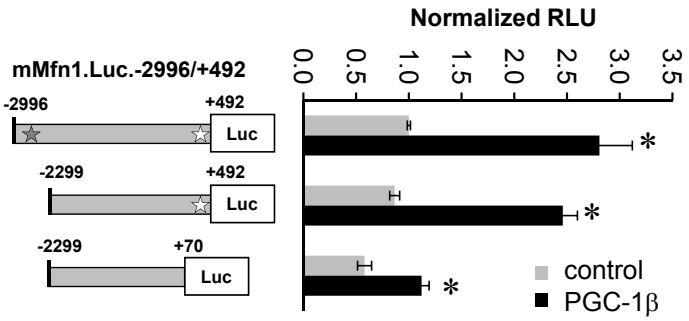

Online Figure VI. PGC-1β activates the *Mfn1* promoter. Serial deletion reporter constructs (mMfn1.Luc series) were cotransfected into C2C12 myocytes with a PGC-1β expression vector (pCATCH-PGC-1β; black bars) or a vector backbone control (pcDNA3.1; gray bars). The bars represent mean luciferase activity (normalized relative light units, RLU) ±SEM. Gray (-2826) and white (+110) stars denote the position of putative ERR sites. *$p<0.05$ compared to empty vector.

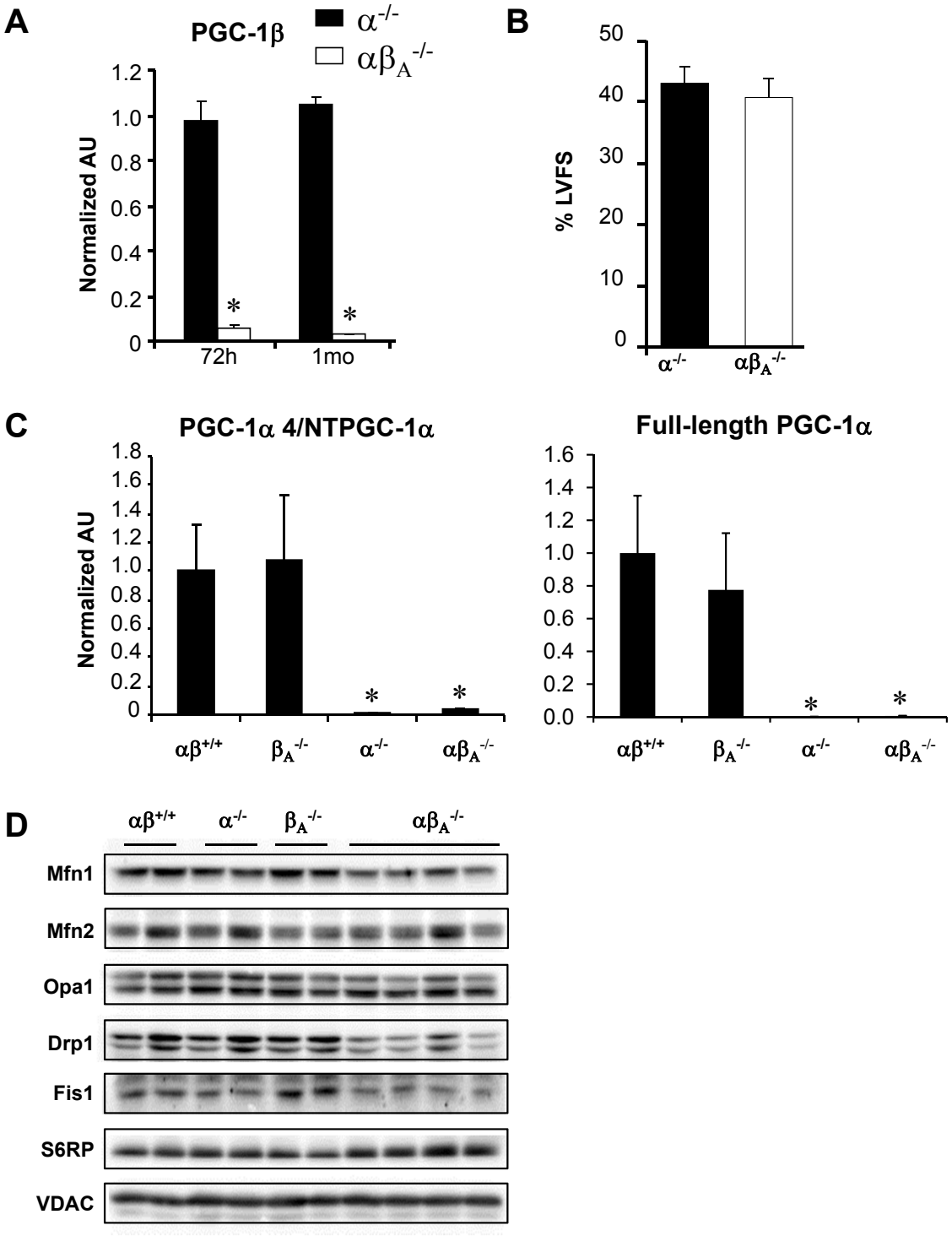

Online Figure VII. PGC-1α$^{-/-}$β$^{f/f/MerCre}$ mice exhibit normal cardiac function. (A) PGC-1β mRNA levels were determined in hearts of PGC-1α$^{-/-}$β$^{f/f/MerCre}$ (αβ$_A^{-/-}$) or control PGC-1α$^{-/-}$ (α$^{-/-}$) mice 72 hours or 1 month after tamoxifen injection. **(B)** Left ventricular fractional shortening (LVFS) in adult heart was determined via echocardiography on 12 week old female PGC-1α$^{-/-}$ (α$^{-/-}$) or PGC-1α$^{-/-}$β$^{f/f/MerCre}$ (αβ$_A^{-/-}$) mice one month after tamoxifen injection. Bars represent mean ±SEM from 4 animals per group. **(C)** Levels of full-length and two alternatively spliced shorter PGC-1α transcripts [PGC-1α4[9] and NT-PGC-1α[10])] in hearts of 2-3 month old PGC-1αβ$^{+/+}$ (αβ$^{+/+}$), PGC-1β$^{f/f/MerCre}$ (β$_A^{-/-}$), PGC-1α$^{-/-}$ (α$^{-/-}$), and PGC-1α$^{-/-}$β$^{f/f/MerCre}$ (αβ$_A^{-/-}$) mice, 1 month after injection of vehicle or tamoxifen (as described in Methods) using qRT-PCR. PGC-1α/NT-PGC-1α primers are in Exon 5 (forward primer) and Exon 7a (reverse primer). Exon 7a is present in PGC-1α4 and NT-PGC-1α, but absent from full-length PGC-1α. Primers for full-length PGC-1α are located in Exon 5 (forward primer) and across the boundary between Exon 6 and 7b (reverse primer). The exon boundary between Exon 6 and 7b exists only in full-length PGC-1α, but not in PGC-1α4 or in NT-PGC-1α. For sequences refer to Supplemental Table 1. **(D)** Representative Western blots assessing levels of fission/fusion proteins in cardiac tissue in 2-3 month old mice across the four genotypes are shown. Samples were taken 1 month after injection with vehicle or tamoxifen (as described in Methods).

Online Table I. Primer Sequences for ChIP and qRT-PCR studies

	Forward	Reverse
Mfn1, rat (ChIP)	TGTGGTTGCTGGGTGACAGT	CGGGTGGATTCCTACCTGGACA
GLUT4, rat (ChIP, -cont)	GACGGACACCTTCT	CCACAGCCTAGCCA
PDK4, rat (ChIP, +cont)	AGATTGGCACCCTTGGGATAGGT	ATGCGTGACATTGAGATGGCTCCT
Mfn1, mouse	AGCCCAACATCTTCATTCTGAA	CTTACAACCTTGAGCTCTTCTACCA
Mfn1, rat	AACTCGGAATCAACGCTGATGAA	ATTCTGGCTCTGAAGCAGAAGCAT
Mfn2, mouse	CATCAGTTACACCGGCTCTAACT	GAGCCTCGACTTTCTTGTTCA
Mfn2, rat	CTCAGGAGCAGCGGGTTTATTGTCT	TGTCGAGGGACCAGCATGTCTATCT
Opa1, mouse	CAGCTGGCAGAAGATCTCAAG	TATGAGCAGGATTTTGACACA
Opa1, rat	CAGCTGGCAGAAGATCTCAAG	CATGAGCAGGATTTTGACACC
Fis1, mouse	ACTGAGCCCCAGAACAAC	TCAGGATTTGGACTTGGAG
Fis1, rat	AAGAGCACGCAGTTTGAATACGCC	TCTTTGCTACCTTTGGGCAACAGC
Drp1, mouse	CTGACGCTTGTGGATTTACC	CCCTTCCCATCAATACATCC
Drp1, rat	AAATGACCCTGCTACATGGAA	AGAAAACCTTGAGATGGATTGG
PGC-1α4/NTPGC-1α, mouse	TCACACCAAACCCACAGAAA	CTGGAAGATATGGCACAT
PGC-1α (full-length), mouse	TGCCATTGTTAAGACCGAG	ACCCTTGGGGTCATTTGG
PGC-1α (all isoforms), mouse	AACCGCAGTCGCAACATG	GTTCGCTCAATAGTCTTGTTCTCA
PGC-1α, rat	CGATGACCCTCCTCACACCA	TTACCTTGAGCATGTTGCG
PGC-1β, mouse	TCCAGAAGTCAGCGGCCTTGTGTCA	CTCTGGGACAGGGCAGCACCGA
PGC-1β, rat	TGGATGAGCTTTCACTGCTGCA	GGTGCCATCCACCTTGACAC
ERRα, mouse	AGGAGTACGTCCTGCTG	CCTCAGCATCTTCAATG
ERRα, rat	TTCGGCGGCTGCAAGCCC	TCCACAGCCTCAGCATCTTCAATGT
Cre	GCCACGACCAAGTGACAGC	TGCACGTTCACCGGCATC
36B4, mouse	ATCCCTGACGCACCGCCGTGA	TGCATCTGCTTGGAGCCCACGTT
36B4, rat	CACCTTCCCACTGGCTGAA	TCCTCCGACTCTTCCTTTGC

Online Table II. Echocardiographic Measurements

Measure	$\alpha\beta^{+/+}$	$\alpha^{-/-}$	$\beta^{-/-}$	$\alpha\beta^{-/-}$
1 week (mixed gender)				
HR (bpm)	448.00 ±24.96	516.75 ±39.56	502.60 ±8.42	445.17 ±11.16
LVPWd (mm)	0.57 ±0.02	0.52 ±0.05	0.64 ±0.05	0.49 ±0.04
LVIDd (mm)	2.31 ±0.07	1.95 ±0.20*	2.20 ±0.12	1.76 ±0.04*
LVPWs	0.85 ±0.04	0.76 ±0.08	0.93 ±0.06	0.66 ±0.05*
LVIDs	1.34 ±0.07	1.13 ±0.18	1.25 ±0.12	1.19 ±0.09
LVM (mg)	29.75 ±2.22	18.64 ±1.70*	31.01 ±5.36	15.43 ±1.23*
LVMI	6.95 ±0.77	4.66 ±0.53	5.25 ±0.60	3.24 ±0.23*
RWT	0.49 ±0.02	0.54 ±0.09	0.54 ±0.03	0.55 ±0.03*
LVFS (%)	42.20 ±1.73	42.87 ±4.45	43.37 ±3.30	32.35 ±4.32*
EF	66.83 ±1.52	68.01 ±8.38	67.81 ±1.58	53.39 ±5.90
CO	3.52 ±0.27	2.53 ±0.19	3.42 ±0.51	1.68 ±0.17*
4 week (females)				
HR (bpm)	532.83 ±15.95	526.86 ±14.77	563.29 ±21.19	490.33 ±18.17
LVPWd (mm)	0.69 ±0.05	0.57 ±0.02*	0.71 ±0.03	0.79 ±0.04
LVIDd (mm)	3.38 ±0.15	3.57 ±0.09	3.34 ±0.05	3.64 ±0.21
LVPWs	1.00 ±0.05	0.89 ±0.04	1.06 ±0.03	0.89 ±0.08
LVIDs	2.11 ±0.18	2.26 ±0.15	1.89 ±0.06	2.92 ±0.26*
LVM (mg)	81.10 ±9.62	63.96 ±4.47	79.01 ±2.66	102.24 ±15.90
LVMI	5.00 ±0.37	4.63 ±0.44	4.57 ±0.05	7.53 ±0.53*
RWT	0.44 ±0.03	0.33 ±0.01*	0.45 ±0.01	0.45 ±0.04
LVFS (%)	37.95 ±2.89	37.06 ±3.16	43.31 ±1.43	20.43 ±3.21*
EF	64.64 ±1.53	63.98 ±4.72	71.99 ±0.87*	40.00 ±3.34*
CO	13.83 ±1.22	13.52 ±1.44	13.23 ±1.12	8.43 ±0.43*
8 week (females)				
HR (bpm)	609.83 ±15.10	523.29 ±28.18*	601.60 ±11.07	516.50 ±17.04*
LVPWd (mm)	0.80 ±0.04	0.62 ±0.05*	0.77 ±0.05	0.72 ±0.03
LVIDd (mm)	3.28 ±0.07	3.62 ±0.12*	3.42 ±0.08	4.58 ±0.20*
LVPWs	1.07 ±0.05	0.93 ±0.07	1.13 ±0.03	0.80 ±0.04*
LVIDs	1.98 ±0.08	2.23 ±0.17	1.97 ±0.06	4.01 ±0.23*
LVM (mg)	84.47 ±3.08	81.55 ±12.01	89.36 ±6.16	140.87 ±8.01*
LVMI	4.27 ±0.24	3.79 ±0.58	3.92 ±0.23	6.79 ±0.36*
RWT	0.50 ±0.03	0.37 ±0.03*	0.47 ±0.03	0.34 ±0.02*
LVFS (%)	39.75 ±1.42	38.74 ±3.30	42.22 ±1.44	12.62 ±1.70*
EF	70.12 ±1.09	63.64 ±2.39*	68.11 ±1.55	23.41 ±1.45*
CO	12.92 ±0.62	14.25 ±1.45	13.83 ±1.68	11.18 ±0.87

*$p<0.05$ relative to $\alpha\beta^{+/+}$
N=4-12 per group

Online Table III. Pathway analysis of Affymetrix GeneChip data from $\alpha\beta^{-/-}$ vs. $\alpha^{-/-}$ mice

Ingenuity Canonical Pathways	p-value
Oxidative Phosphorylation	3.98E-63
Mitochondrial Dysfunction	3.16E-49
Ubiquinone Biosynthesis	1.26E-33
Valine, Leucine and Isoleucine Degradation	2.51E-20
Citrate Cycle	1.00E-18
Propanoate Metabolism	3.98E-14
Butanoate Metabolism	7.94E-12
Pyruvate Metabolism	1.02E-07
Alanine and Aspartate Metabolism	1.17E-07
β-alanine Metabolism	2.00E-07
Glycolysis/Gluconeogenesis	1.55E-05
Phenylalanine, Tyrosine and Tryptophan Biosynthesis	6.31E-05
Lysine Degradation	9.77E-05
Fatty Acid Metabolism	1.95E-04
Arginine and Proline Metabolism	4.17E-04
NRF2-mediated Oxidative Stress Response	4.90E-04
Tryptophan Metabolism	5.25E-04
Synthesis and Degradation of Ketone Bodies	8.71E-04
Ascorbate and Aldarate Metabolism	1.29E-03
Purine Metabolism	1.38E-03
Aryl Hydrocarbon Receptor Signaling	3.63E-03
Nucleotide Sugars Metabolism	5.13E-03
Pentose and Glucuronate Interconversions	6.03E-03
Glyoxylate and Dicarboxylate Metabolism	7.59E-03
Tyrosine Metabolism	9.33E-03
Stilbene, Coumarine and Lignin Biosynthesis	9.33E-03
Phenylalanine Metabolism	1.02E-02
Aldosterone Signaling in Epithelial Cells	1.07E-02
Glycine, Serine and Threonine Metabolism	1.35E-02
Valine, Leucine and Isoleucine Biosynthesis	1.35E-02
Glutamate Metabolism	2.19E-02
LPS/IL-1 Mediated Inhibition of RXR Function	2.82E-02
Histidine Metabolism	2.88E-02
Cholecystokinin/Gastrin-mediated Signaling	3.63E-02
G Beta Gamma Signaling	4.57E-02
Chemokine Signaling	4.68E-02
VEGF Signaling	4.79E-02

$p<0.05$ was used as a cutoff

Online Table IV. Pathway analysis of Affymetrix GeneChip data from $\alpha\beta^{-/-}$ vs. $\alpha^{-/-}$ mice

Fatty Acid Metabolism		
Symbol	Entrez Gene Name	Fold Change
ACAD11	acyl-CoA dehydrogenase family, member 11	-1.333
ACADS	acyl-CoA dehydrogenase, C-2 to C-3 short chain	-1.248
ACADSB	acyl-CoA dehydrogenase, short/branched chain	-1.435
ACADVL	acyl-CoA dehydrogenase, very long chain	-1.580
ADHFE1	alcohol dehydrogenase, iron containing, 1	-1.383
ALDH1A2	aldehyde dehydrogenase 1 family, member A2	1.550
ALDH2	aldehyde dehydrogenase 2 family (mitochondrial)	-1.245
ALDH4A1	aldehyde dehydrogenase 4 family, member A1	-1.318
AUH	AU RNA binding protein/enoyl-CoA hydratase	-1.449
ECHS1	enoyl CoA hydratase, short chain, 1, mitochondrial	-1.786
EHHADH	enoyl-CoA, hydratase/3-hydroxyacyl CoA dehydrogenase	-1.495
GCDH	glutaryl-CoA dehydrogenase	-1.401
HADH	hydroxyacyl-CoA dehydrogenase	-1.242
SLC27A1	16	-1.370
Citric Acid Cycle		
Symbol	Entrez Gene Name	Fold Change
ACO2	aconitase 2, mitochondrial	-1.595
CLYBL	citrate lyase beta like	-1.258
CS	citrate synthase	-1.297
Csl	citrate synthase like	-1.280
DLD	dihydrolipoamide dehydrogenase	-1.905
DLST	dihydrolipoamide S-succinyltransferase (E2 component of 2-oxo-glutarate complex)	-2.119
FH	fumarate hydratase	-1.869
IDH2	isocitrate dehydrogenase 2 (NADP+), mitochondrial	-1.258
IDH3A	isocitrate dehydrogenase 3 (NAD+) alpha	-1.399
IDH3B	isocitrate dehydrogenase 3 (NAD+) beta	-1.965
IDH3G	isocitrate dehydrogenase 3 (NAD+) gamma	-1.536
MDH2	malate dehydrogenase 2, NAD (mitochondrial)	-1.689
OGDH	oxoglutarate (alpha-ketoglutarate) dehydrogenase (lipoamide)	-1.326
PC	pyruvate carboxylase	-1.271
SDHA	succinate dehydrogenase complex, subunit A, flavoprotein (Fp)	-1.828
SDHB	succinate dehydrogenase complex, subunit B, iron sulfur (Ip)	-2.398
SDHC	succinate dehydrogenase complex, subunit C, integral membrane protein, 15kDa	-1.880
SDHD	succinate dehydrogenase complex, subunit D, integral membrane protein	-2.257
SUCLA2	succinate-CoA ligase, ADP-forming, beta subunit	-1.473
SUCLG1	succinate-CoA ligase, alpha subunit	-1.792
Oxidative Phosphorylation		
Symbol	Entrez Gene Name	Fold Change
ATP5A1	ATP synthase, H+ transporting, mitochondrial F1 complex, alpha subunit 1, cardiac muscle	-1.495
ATP5C1	ATP synthase, H+ transporting, mitochondrial F1 complex, gamma polypeptide 1	-1.642
ATP5D	ATP synthase, H+ transporting, mitochondrial F1 complex, delta subunit	-1.353
ATP5E	ATP synthase, H+ transporting, mitochondrial F1 complex, epsilon subunit	-1.701
ATP5F1	ATP synthase, H+ transporting, mitochondrial Fo complex, subunit B1	-1.730
ATP5G1	ATP synthase, H+ transporting, mitochondrial Fo complex, subunit C1 (subunit 9)	-1.529
ATP5G3	ATP synthase, H+ transporting, mitochondrial Fo complex, subunit C3 (subunit 9)	-1.828
ATP5I	ATP synthase, H+ transporting, mitochondrial Fo complex, subunit E	-2.632
ATP5J2	ATP synthase, H+ transporting, mitochondrial Fo complex, subunit F2	-1.403
ATP5O	ATP synthase, H+ transporting, mitochondrial F1 complex, O subunit	-2.237
COX10	cytochrome c oxidase assembly homolog 10 (yeast)	-1.684
COX4I1	cytochrome c oxidase subunit IV isoform 1	-1.996
COX5A	cytochrome c oxidase subunit Va	-1.502
COX5B	cytochrome c oxidase subunit Vb	-1.770
COX6A1	cytochrome c oxidase subunit VIa polypeptide 1	-1.435
COX6B1	cytochrome c oxidase subunit VIb polypeptide 1 (ubiquitous)	-1.626
COX7A1	cytochrome c oxidase subunit VIIa polypeptide 1 (muscle)	-1.323
COX7A2	cytochrome c oxidase subunit VIIa polypeptide 2 (liver)	-1.730
COX8A	cytochrome c oxidase subunit VIIIA (ubiquitous)	-1.637
CYC1	cytochrome c-1	-2.222
NDUFA1	NADH dehydrogenase (ubiquinone) 1 alpha subcomplex, 1, 7.5kDa	-1.805
NDUFA11	NADH dehydrogenase (ubiquinone) 1 alpha subcomplex, 11, 14.7kDa	-1.266
NDUFA12	NADH dehydrogenase (ubiquinone) 1 alpha subcomplex, 12	-1.565
NDUFA13	NADH dehydrogenase (ubiquinone) 1 alpha subcomplex, 13	-1.493
NDUFA2	NADH dehydrogenase (ubiquinone) 1 alpha subcomplex, 2, 8kDa	-1.357
NDUFA4	NADH dehydrogenase (ubiquinone) 1 alpha subcomplex, 4, 9kDa	-1.949
NDUFA5	NADH dehydrogenase (ubiquinone) 1 alpha subcomplex, 5, 13kDa	-2.347

NDUFA7	NADH dehydrogenase (ubiquinone) 1 alpha subcomplex, 7, 14.5kDa	-1.323
NDUFA8	NADH dehydrogenase (ubiquinone) 1 alpha subcomplex, 8, 19kDa	-1.779
NDUFA9	NADH dehydrogenase (ubiquinone) 1 alpha subcomplex, 9, 39kDa	-2.088
NDUFAB1	NADH dehydrogenase (ubiquinone) 1, alpha/beta subcomplex, 1, 8kDa	-2.016
NDUFB10	NADH dehydrogenase (ubiquinone) 1 beta subcomplex, 10, 22kDa	-2.114
NDUFB11	NADH dehydrogenase (ubiquinone) 1 beta subcomplex, 11, 17.3kDa	-1.276
NDUFB2	NADH dehydrogenase (ubiquinone) 1 beta subcomplex, 2, 8kDa	-1.473
NDUFB3	NADH dehydrogenase (ubiquinone) 1 beta subcomplex, 3, 12kDa	-1.701
NDUFB6	NADH dehydrogenase (ubiquinone) 1 beta subcomplex, 6, 17kDa	-1.555
NDUFB7	NADH dehydrogenase (ubiquinone) 1 beta subcomplex, 7, 18kDa	-2.020
NDUFB8	NADH dehydrogenase (ubiquinone) 1 beta subcomplex, 8, 19kDa	-2.299
NDUFB9	NADH dehydrogenase (ubiquinone) 1 beta subcomplex, 9, 22kDa	-1.927
NDUFC1	NADH dehydrogenase (ubiquinone) 1, subcomplex unknown, 1, 6kDa	-1.437
NDUFC2	NADH dehydrogenase (ubiquinone) 1, subcomplex unknown, 2, 14.5kDa	-1.414
NDUFS1	NADH dehydrogenase (ubiquinone) Fe-S protein 1, 75kDa (NADH-coenzyme Q reductase)	-2.083
NDUFS2	NADH dehydrogenase (ubiquinone) Fe-S protein 2, 49kDa (NADH-coenzyme Q reductase)	-1.957
NDUFS3	NADH dehydrogenase (ubiquinone) Fe-S protein 3, 30kDa (NADH-coenzyme Q reductase)	-1.718
NDUFS4	NADH dehydrogenase (ubiquinone) Fe-S protein 4, 18kDa (NADH-coenzyme Q reductase)	-1.477
NDUFS5	NADH dehydrogenase (ubiquinone) Fe-S protein 5, 15kDa (NADH-coenzyme Q reductase)	-1.376
NDUFS6	NADH dehydrogenase (ubiquinone) Fe-S protein 6, 13kDa (NADH-coenzyme Q reductase)	-1.460
NDUFS7	NADH dehydrogenase (ubiquinone) Fe-S protein 7, 20kDa (NADH-coenzyme Q reductase)	-1.304
NDUFS8	NADH dehydrogenase (ubiquinone) Fe-S protein 8, 23kDa (NADH-coenzyme Q reductase)	-1.603
NDUFV1	NADH dehydrogenase (ubiquinone) flavoprotein 1, 51kDa	-2.227
NDUFV2	NADH dehydrogenase (ubiquinone) flavoprotein 2, 24kDa	-1.490
NDUFV3	NADH dehydrogenase (ubiquinone) flavoprotein 3, 10kDa	-1.282
PPA2	pyrophosphatase (inorganic) 2	-1.408
SDHA	succinate dehydrogenase complex, subunit A, flavoprotein (Fp)	-1.828
SDHB	succinate dehydrogenase complex, subunit B, iron sulfur (Ip)	-2.398
SDHC	succinate dehydrogenase complex, subunit C, integral membrane protein, 15kDa	-1.880
SDHD	succinate dehydrogenase complex, subunit D, integral membrane protein	-2.257
UQCR10	ubiquinol-cytochrome c reductase, complex III subunit X	-1.626
UQCR11	ubiquinol-cytochrome c reductase, complex III subunit XI	-1.996
UQCRC1	ubiquinol-cytochrome c reductase core protein I	-1.792
UQCRC2	ubiquinol-cytochrome c reductase core protein II	-1.645
UQCRFS1	ubiquinol-cytochrome c reductase, Rieske iron-sulfur polypeptide 1	-2.227
UQCRHL	ubiquinol-cytochrome c reductase hinge protein	-2.041
UQCRQ	ubiquinol-cytochrome c reductase, complex III subunit VII, 9.5kDa	-2.110

Supplemental References

1. Zechner C, Lai L, Zechner JF, Geng T, Yan Z, Rumsey JW, Collia D, Chen Z, Wozniak DF, Leone TC, Kelly DP. Total skeletal muscle PGC-1 deficiency uncouples mitochondrial derangements from fiber type determination and insulin sensitivity. *Cell Metab*. 2010;12:633-642.
2. Lai L, Leone TC, Zechner C, Schaeffer PJ, Kelly SM, Flanagan DP, Medeiros DM, Kovacs A, Kelly DP. Transcriptional coactivators PGC-1alpha and PGC-lbeta control overlapping programs required for perinatal maturation of the heart. *Genes Dev.* 2008;22:1948-1961.
3. Bruning JC, Michael MD, Winnay JN, Hayashi T, Horsch D, Accili D, Goodyear LJ, Kahn CR. A muscle-specific insulin receptor knockout exhibits features of the metabolic syndrome of NIDDM without altering glucose tolerance. *Mol Cell*. 1998;2:559-569.
4. Leone TC, Lehman JJ, Finck BN, Schaeffer PJ, Wende AR, Boudina S, Courtois M, Wozniak DF, Sambandam N, Bernal-Mizrachi C, Chen Z, Holloszy JO, Medeiros DM, Schmidt RE, Saffitz JE, Abel ED, Semenkovich CF, Kelly DP. PGC-1alpha deficiency causes multi-system energy metabolic derangements: Muscle dysfunction, abnormal weight control and hepatic steatosis. *PLoS Biol*. 2005;3:e101.
5. Sahn DJ, DeMaria A, Kisslo J, Weyman A. Recommendations regarding quantitation in M-mode echocardiography: Results of a survey of echocardiographic measurements. *Circulation*. 1978;58:1072-1083.
6. Gardin JM, Siri FM, Kitsis RN, Edwards JG, Leinwand LA. Echocardiographic assessment of left ventricular mass and systolic function in mice. *Circ Res*. 1995;76:907-914.
7. Oh JK, Seward JB, Takjik AJ. *The Echo Manual*. Philadelphia, PA: Lippincott Williams and Wilkins; 1999.
8. Boehm EA, Jones BE, Radda GK, Veech RL, Clarke K. Increased uncoupling proteins and decreased efficiency in palmitate-perfused hyperthyroid rat heart. *Am J Physiol Heart Circ Physiol*. 2001;280:H977-983.
9. Schaeffer PJ, Desantiago J, Yang J, Flagg TP, Kovacs A, Weinheimer CJ, Courtois M, Leone TC, Nichols CG, Bers DM, Kelly DP. Impaired contractile function and calcium handling in hearts of cardiac-specific calcineurin b1-deficient mice. *Am J Physiol Heart Circ Physiol*. 2009;297:H1263-1273.
10. Saks VA, Veksler VI, Kuznetsov AV, Kay L, Sikk P, Tiivel T, Tranqui L, Olivares J, Winkler K, Wiedemann F, Kunz WS. Permeabilized cell and skinned fiber techniques in studies of mitochondrial function in vivo. *Mol Cell Biochem*. 1998;184:81-100.
11. Frith MC, Fu Y, Yu L, Chen JF, Hansen U, Weng Z. Detection of functional DNA motifs via statistical over-representation. *Nucleic Acids Res*. 2004;32:1372-1381.
12. Huss JM, Torra IP, Staels B, Giguere V, Kelly DP. Estrogen-related receptor alpha directs peroxisome proliferator-activated receptor alpha signaling in the transcriptional control of energy metabolism in cardiac and skeletal muscle. *Mol Cell Biol*. 2004;24:9079-9091.
13. Taegtmeyer H, Overturf ML. Effects of moderate hypertension on cardiac function and metabolism in the rabbit. *Hypertension*. 1988;11:416-426.
14. Pagliarini DJ, Calvo SE, Chang B, Sheth SA, Vafai SB, Ong SE, Walford GA, Sugiana C, Boneh A, Chen WK, Hill DE, Vidal M, Evans JG, Thorburn DR, Carr SA, Mootha VK. A mitochondrial protein compendium elucidates complex I disease biology. *Cell*. 2008;134:112-123.
15. Koo SH, Satoh H, Herzig S, Lee CH, Hedrick S, Kulkarni R, Evans RM, Olefsky J, Montminy M. PGC-1 promotes insulin resistance in liver through PPAR-alpha-dependent induction of TRB-3. *Nat Med*. 2004;10:530-534.
16. Lin J, Yang R, Tarr PT, Wu PH, Handschin C, Li S, Yang W, Pei L, Uldry M, Tontonoz P, Newgard CB, Spiegelman BM. Hyperlipidemic effects of dietary saturated fats mediated through PGC-1beta coactivation of SREBP. *Cell*. 2005;120:261-273.

17. Gaillard S, Grasfeder LL, Haeffele CL, Lobenhofer EK, Chu TM, Wolfinger R, Kazmin D, Koves TR, Muoio DM, Chang CY, McDonnell DP. Receptor-selective coactivators as tools to define the biology of specific receptor-coactivator pairs. *Mol Cell*. 2006;24:797-803.
18. Sebastian D, Hernandez-Alvarez MI, Segales J, Sorianello E, Munoz JP, Sala D, Waget A, Liesa M, Paz JC, Gopalacharyulu P, Oresic M, Pich S, Burcelin R, Palacin M, Zorzano A. Mitofusin 2 (Mfn2) links mitochondrial and endoplasmic reticulum function with insulin signaling and is essential for normal glucose homeostasis. *Proc Natl Acad Sci USA*. 2012;109:5523-5528.
19. Huss JM, Kopp RP, Kelly DP. Peroxisome proliferator-activated receptor coactivator-1alpha (PGC-1alpha) coactivates the cardiac-enriched nuclear receptors estrogen-related receptor-alpha and -gamma. Identification of novel leucine-rich interaction motif within PGC-1alpha. *J Biol Chem*. 2002;277:40265-40274.
20. Vega RB, Huss JM, Kelly DP. The coactivator PGC-1 cooperates with peroxisome proliferator-activated receptor alpha in transcriptional control of nuclear genes encoding mitochondrial fatty acid oxidation enzymes. *Mol Cell Biol*. 2000;20:1868-1876.
21. Lin J, Puigserver P, Donovan J, Tarr P, Spiegelman BM. Peroxisome proliferator-activated receptor gamma coactivator 1beta (PGC-1beta), a novel PGC-1-related transcription coactivator associated with host cell factor. *J Biol Chem*. 2002;277:1645-1648.
22. Wende AR, Huss JM, Schaeffer PJ, Giguere V, Kelly DP. PGC-1alpha coactivates PDK4 gene expression via the orphan nuclear receptor ERRalpha: A mechanism for transcriptional control of muscle glucose metabolism. *Mol Cell Biol*. 2005;25:10684-10694.
23. Yang J, Williams RS, Kelly DP. Bcl3 interacts cooperatively with peroxisome proliferator-activated receptor gamma (PPARgamma) coactivator 1alpha to coactivate nuclear receptors estrogen-related receptor alpha and PPARalpha. *Mol Cell Biol*. 2009;29:4091-4102.
24. Lehman JJ, Barger PM, Kovacs A, Saffitz JE, Medeiros DM, Kelly DP. Peroxisome proliferator-activated receptor gamma coactivator-1 promotes cardiac mitochondrial biogenesis. *J Clin Invest*. 2000;106:847-856.
25. Cresci S, Wright LD, Spratt JA, Briggs FN, Kelly DP. Activation of a novel metabolic gene regulatory pathway by chronic stimulation of skeletal muscle. *Am J Physiol*. 1996;270:C1413-1420.
26. Schilling J, Lai L, Sambandam N, Dey CE, Leone TC, Kelly DP. Toll-like receptor-mediated inflammatory signaling reprograms cardiac energy metabolism by repressing peroxisome proliferator-activated receptor gamma coactivator-1 signaling. *Circ Heart Fail*. 2011;4:474-482.